Available online at www.sciencedirect.com
ScienceDirect
Dyes and Pigments 77 (2008) 564–569
DYES and PIGMENTS
www.elsevier.com/locate/dyepig

The synthesis and electro-optic properties of polyimide/silica hybrids containing the benzothiazole chromophore

Fengxian Qiu [a,c,*], Zulin Da [a], Dongya Yang [a], Guorong Cao [b], Pingping Li [c]

[a] School of Chemistry and Chemical Engineering, Jiangsu University, Zhenjiang 212013, China
[b] Faculty of Science, Jiangsu University, Zhenjiang 212013, China
[c] Jiangsu Provincial Key Laboratory of Modern Agricultural Equipment and Technology, Zhenjiang 212013, China

Received 16 May 2007; received in revised form 2 August 2007; accepted 9 August 2007
Available online 6 September 2007

Abstract

A series of polyimide/silica NLO hybrid materials were synthesized from pyromellitic dianhydride, 2,2-bis(3-amino-4-hydroxyphenyl) hexafluoropropane, nonlinear optical molecule 4-(*N*-2-hydroxyethyl-*N*-methylamino)-4′-[(6-nitrobenzothiazol-2-yl)diazenyl]azobenzene via a sol–gel process; the tetraethoxysilane content in the hybrid films was varied from 0 to 22.5%. The prepared polyimide/silica hybrids were characterized by FT-IR, differential scanning calorimeter, thermogravimetric analysis, scanning electron microscopy, transmission electron microscope and X-ray diffraction. The glass transition temperature and decomposition temperature at 5% mass loss were in the range 214–360 °C and 317–428 °C, respectively, showing that the hybrid materials had excellent thermal stability. Polymer solutions were spin-coated on indium–tin-oxide glass, forming optical quality thin films. The electro-optic coefficients at 832 nm for poled polymer thin films were ≈20 to 33 pm/V and the values were retained >88% for more than 100 h. The experimental results suggest that the hybrid thin films have potential applications as passive films for optical devices.

Keywords: Nonlinear optical (NLO); Polyimide; Electro-optic properties

1. Introduction

A large number of nonlinear optical (NLO) polymers have been developed for optical devices such as waveguides [1,2] and optical modulators [3], and for optical applications such as optical memory storage [4] and holography [5]. Some materials with two-photon absorption (2PA) and donor–acceptor structure were synthesized. Their ultrafast response and the nonlinear optical properties were studied [6,7]. Recently, inorganic/organic hybrid NLO materials, prepared by sol–gel processing, have received much attention [8–10]. The sol–gel technology arises as a method of fabrication of high quality oxide materials and is well adapted for thin film deposition [11]. This process also offers an attractive route to fabricate hybrid materials with high thermal stability, excellent optical quality and high stability of dipole alignment by locking the chromophore in the silica networks.

In this study, we synthesized a polyimide via a Mitsunobu reaction [12–14]. Then, using coupling agent, 3-aminopropyltriethoxysilane (APTES), a combination of two different components namely amino (organic) and silicon alkoxy (inorganic) groups, reacted with polyimide to form precursors containing alkoxysilane. Therefore, this compound had the ability to form simultaneously an organic network through ring-opening polyaddition of polyimide and an inorganic SiO_2 network through hydrolysis and subsequent condensation reaction of alkoxy groups [15]. At last, the hybrids were prepared with tetraethoxysilane (TEOS) by sol–gel method. SiO_2 had remarkably high thermal stability and its introduction improved the thermal stability [16].

* Corresponding author. School of Chemistry and Chemical Engineering, Jiangsu University, Zhenjiang 212013, China. Tel.: +86 51188617407.
E-mail address: fxqiuchem@163.com (F.X. Qiu).

0143-7208/$ - see front matter © 2007 Elsevier Ltd. All rights reserved.
doi:10.1016/j.dyepig.2007.08.012

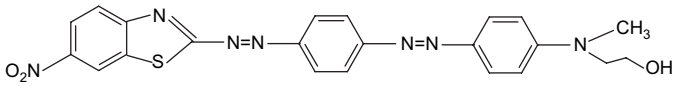

Fig. 1. Chemical structure of the NLO chromophore HNBDA.

2. Experimental

N,*N*-Dimethylacetamide (DMAC) was stirred over powdered calcium hydride overnight and then distilled under reduced pressure and stored over 4 Å molecular sieves. 2,2-Bis(3-amino-4-hydroxyphenyl) hexafluoro propane (6FHP) was obtained from TCI and used without further purification. Pyromellitic dianhydride (PMDA) was obtained from Beijing chemistry agent plant. 3-Aminopropyltriethoxysilane, APTES, was purchased from Nanjing Shuguang Chemical Plant. Tetrahydrofuran (THF) was purified by distillation and other reagents and solvents were obtained commercially and were used as received. 4-(*N*-2-Hydroxyethyl-*N*-methylamino)-4′-[(6-nitrobenzothiazol-2-yl)diazenyl]azobenzene (HNBDA) was prepared by our group.

2.1. Preparation of polyimide/SiO_2 hybrid materials

Polymerization was conducted in a three-neck flask. A stoichiometric amount of PMDA (7.5 mmol) was added to a solution of 6FHP (7.5 mmol) in 30 mL DMAC at 0 °C. The solution was then warmed to room temperature and magnetically stirred overnight under nitrogen. PPh_3 (1.5 mmol) and NLO chromophore 4-(*N*-2-hydroxyethyl-*N*-methylamino)-4′-[(6-nitrobenzothiazol-2-yl)diazenyl]azobenzene (HNBDA, see Fig. 1) (1.50 mmol) were dissolved in THF (15 mL) and added dropwise into the solution. The reaction mixture was stirred for 2 days at room temperature and the pure polyimide was obtained and then, APTES was added to PI and allowed to react for 4 h. Various ratios of TEOS were added to mixture as shown in Table 1. After 12 h of reaction, the homogeneous transparent sol could be obtained. Then the resulting homogeneous solution was transferred to a conical flask and was sealed by plastic film. After the homogeneous sol was dried for 5 days and opened several small holes and evaporated the solvent slowly. The homogeneous transparent gel was formed. Then the sample was heated at 110 °C under vacuum for 2 h to remove residual solvent and by-products (water, alcohol, etc.). The hybrid materials were obtained. The synthetic route is shown in Fig. 2.

2.2. Characterization of polyimide/SiO_2 hybrid materials

FT-IR spectra of the prepared thin films were obtained on a KBr pellet using Nicolet AVATAR 360 spectrometer. The optical characteristics of materials were measured in Shimadzu UV-240. The fracture surface of hybrid was examined on the SIRION scanning electron microscope (SEM). HITACHI H-600 transmission electron microscope (TEM) was used to measure the particle sizes. Thermogravimetric analysis (TGA) and differential scanning calorimetry (DSC) were performed on NETZSCH STA449C. X-ray diffraction (XRD) pattern of SiO_2 was obtained with a Cu Kα X-ray source and a step of 0.02 (2θ).

3. Results and discussion

Fig. 3 illustrated the FT-IR spectra of the prepared hybrids pH-1 and pH-3. From the spectra, the imide absorptions were at 730, 1375, 1720, 1788 cm^{-1}. The absorption band at around 1055–1150 cm^{-1} gradually increased in intensity with the increase in silica contents, consistent with the formation of the three-dimensional Si–O–Si network in the hybrids [17,18]. The broad absorption at around 3100–3300 cm^{-1} was assigned to the Si–OH residue, formed in the hydrolysis of alkoxy groups of TEOS. Besides, the FT-IR spectra consisted of some peaks located at 1516 cm^{-1} (ν_{as}, –N=N–), 1250, 1520 cm^{-1} (ν_s, $-NO_2$), 1148 cm^{-1} (C=S), 1377 cm^{-1} (wagging CH_2), 1728 cm^{-1} (ν_{as}, –C=O).

Figs. 4 and 5 showed the SEM and TEM micrographs of the prepared polyimide/silica hybrids. In most cases, surface morphology of materials was of great importance for many technical applications requiring well-defined surfaces or interfaces. From Fig. 4, no phase separation could be observed. That is, covalent bonding (Si–O–Si) between the organic and inorganic components enhanced miscibility. They were homogeneously and uniformly dispersed at a molecular level. When the silica content was below 15 wt%, the silica particle size was 50 nm, as shown in Fig. 5. However, when the silica content was increased to 22.5 wt%, the particle size increased to 68 nm. The increase in the silica particle size clearly resulted from the increase in the aggregation tendency as the silica content and the number of silica particles were increased. These micrographs showed the fine interconnected or co-continuous

Table 1
Reactant summary and properties of materials

Hybrid material	TEOS (wt%)	APTES (mL)	HCl (mL)	H_2O (mL)	THF (mL)	T_g[a] (°C)	T_d[b] (°C)	γ_{33} (pm/V)	$\gamma_{(t)}/\gamma_0$ (%, 100 h)	Appearance[c] (Transmittance at 832 nm)
Pure PI	0					214	317	33	90	
pH-1	5	0.20	0.10	0.25	30	328	408	26	90	Transparent (99.9%)
pH-2	10	0.20	0.25	0.53	30	334	414	22	89	Transparent (99.7%)
pH-3	15	0.20	0.50	1.02	30	338	420	21	88	Transparent (99.5%)
pH-4	22.5	0.20	0.65	2.10	30	360	428	20	88	Semi-transparent (94.3%)

[a] Experimental results from DSC curves.
[b] Experimental results from TGA curves at 5% mass loss.
[c] UV–vis spectra were observed.

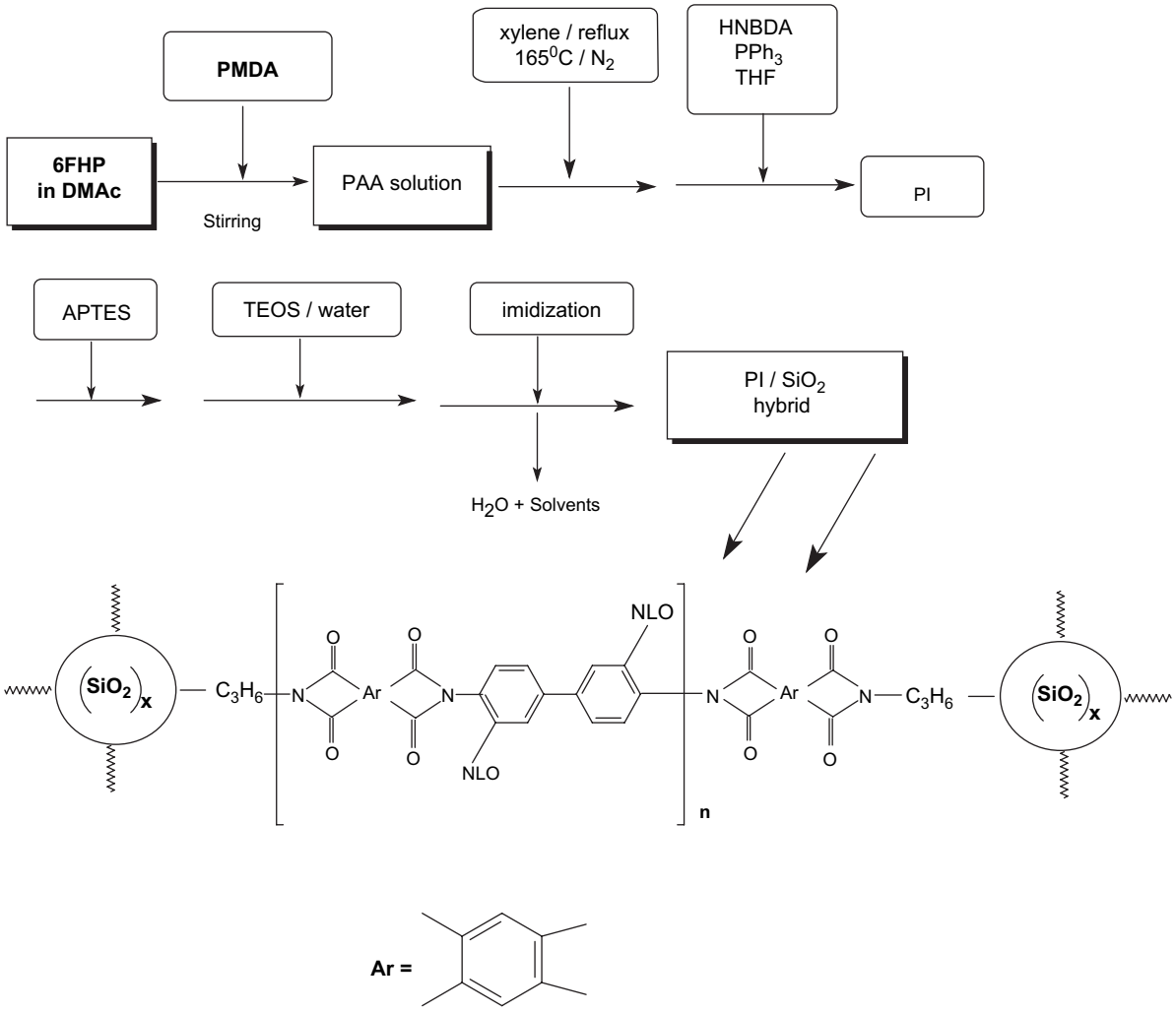

Fig. 2. Reaction scheme for preparing NLO hybrids.

phases' morphology, which improved the efficiency of stress transfer mechanisms between the two components.

An attempt for homogeneity was made to estimate the crystallinity of hybrids by the powder XRD measurement. From Fig. 6, the diffraction pattern of pH-2 was featureless, showing only broad amorphous halos at $2\theta = 23.54°$, deriving from homogeneously silica matrix. The reason was also that covalent bonding (Si–O–Si) between the organic and inorganic components enhanced the miscibility.

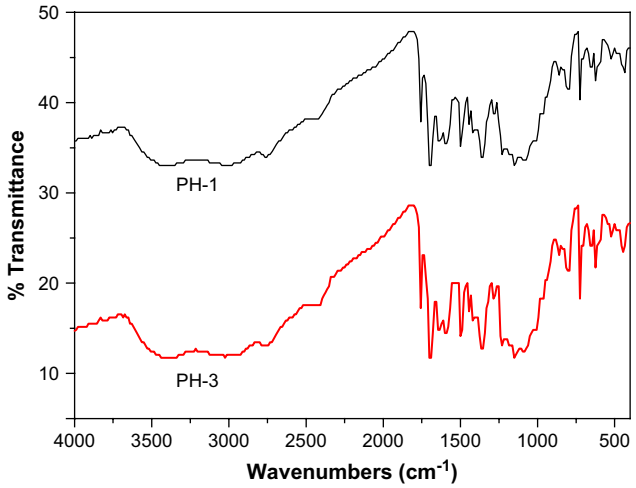

Fig. 3. FT-IR spectra of hybrids.

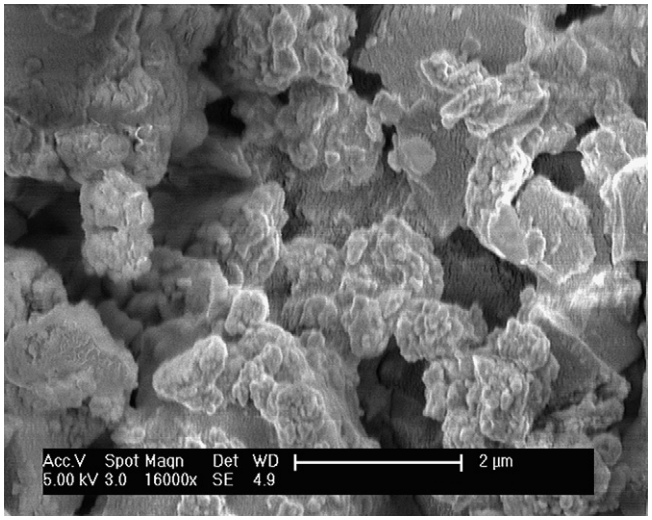

Fig. 4. SEM photograph of pH-2.

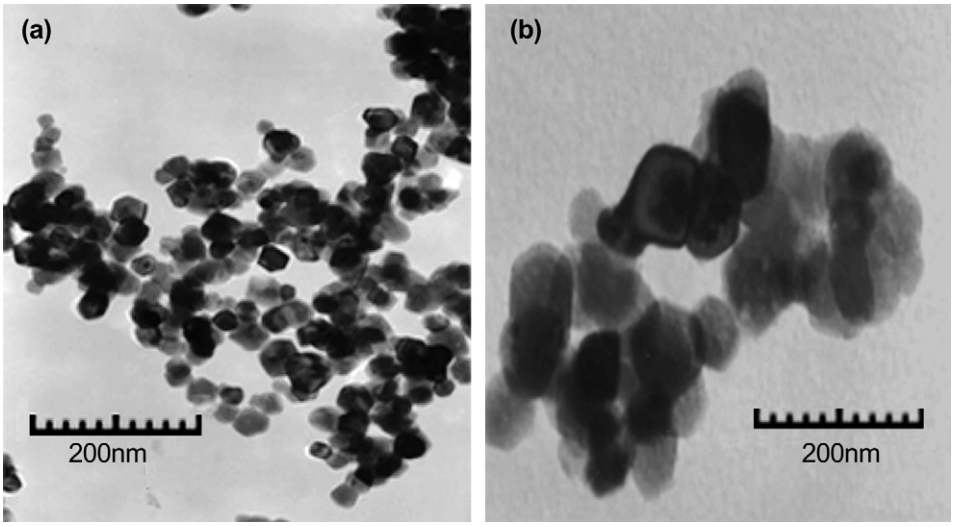

Fig. 5. TEM photographs of pH-2(a) and pH-4(b).

To examine thermal activities of hybrid materials, DSC and TGA experiments were carried out on NETZSCH STA449C with the heating rate of 10 °C/min under nitrogen (Figs. 7 and 8). The data of the thermal decomposition temperature (T_d) are listed in Table 1. They were all above 400 °C for hybrids. It suggested the successful incorporation of the silica moiety in the hybrid materials. The glass transition temperature (T_g) of hybrids increased with the increase of TEOS content (see Table 1). The results clearly showed that T_g and T_d at 5% mass loss of composite were higher than that of pure polyimide, which was attributed to the formation of the silicon crosslink network. This was also clearly caused by the strong interaction between the SiO_2 and the PI, which limited the segmental movement of the PI. It was estimated that these materials would be pretty good for practical application. UV–vis absorption was used to characterize the transparency of hybrids. The results at 832 nm are listed in Table 1.

A reflective EO polymer light modulator was fabricated using PI or hybrid as the EO material. The test sample consisted of a high-index prism, a thin silver film, a poled material layer, a buffer layer, and a base gold film. The silver film was thermally evaporated onto the hypotenuse face of a high-index prism as the first electrode. A material was spin-coated onto the silver substrate to a thickness of 1–2 μm, which can support four or five surface-plasmon modes with TE or TM polarization. A polymer buffer layer was then coated onto the PI or hybrid film to a thickness of 5.68 μm. Finally, a gold film was deposited onto the buffer layer as the base electrode. The electro-optical characterization of the PI or hybrid layer in the EO modulator was conducted by an improved ATR technique. The electro-optic coefficient (γ_{33}) of the EO polymer layer in the EO modulator can be determined according to the following equation:

$$\gamma_{33} = -\frac{2n_1 \cos\theta}{kn_3^3 E}\Delta I \quad (1)$$

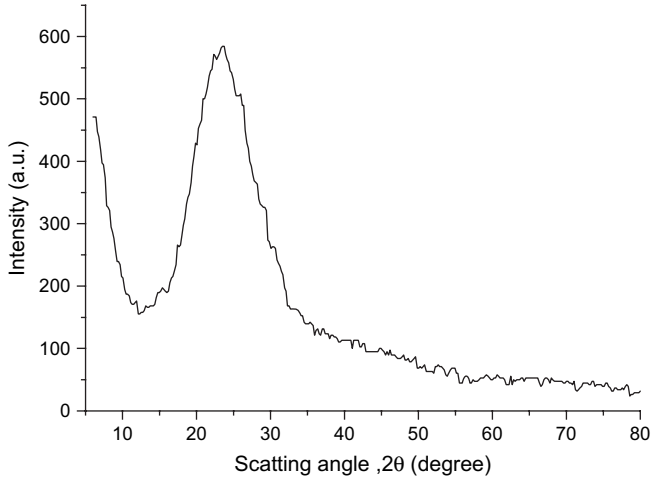

Fig. 6. XRD pattern of pH-2.

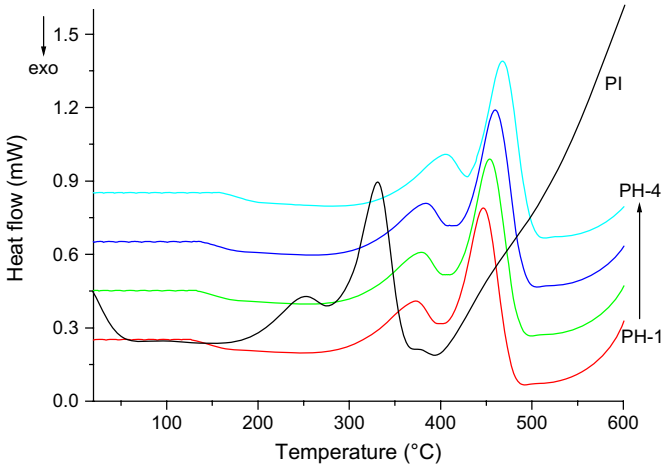

Fig. 7. DSC curves of PI and hybrids.

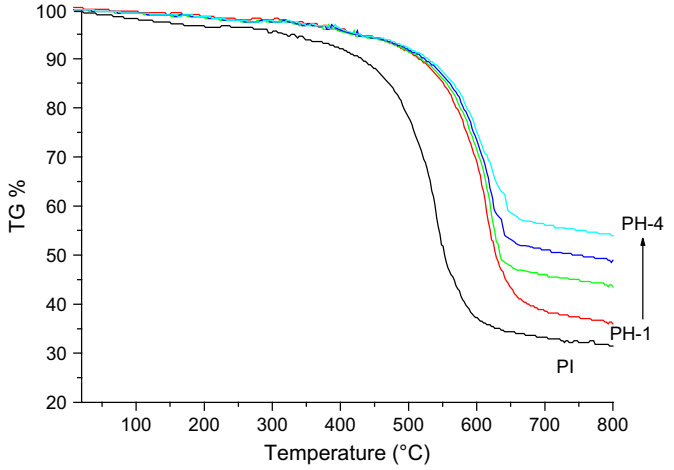

Fig. 8. TGA curves of PI and hybrids.

where γ_{33} is the EO coefficient of the polymer, n_1 and n_3 are the refractive indices of the prism and the PI or hybrid film, respectively, E is the applied electric field, ΔI is the modulated light intensity, θ is the light incident angle which is defined as the modulator's working interior angle and k is the slope value of the fall-off of the ATR resonance dip [19]. The electro-optic (EO) coefficient measurement of our hybrid was performed at a wavelength of 832 nm. The γ_{33} values are listed in Table 1. From Table 1, the thermal stability of hybrid was higher than the corresponding pure polyimide but the γ_{33} coefficients of hybrids were smaller than the corresponding polyimide. This was due to the content of chromophore that was smaller than the pure polyimide. Moreover, the EO coefficient could be further enhanced through modification of the NLO chromophore, increasing the NLO chromophore concentration and/or optimization of the poling process to achieve larger orientation degree of the chromophore dipole moments. The thermal alignment stability of these polyimides and hybrids was investigated by in situ EO coefficients measured using the heater mounted sample holder. The initial values of hybrids pH-1, pH-2, pH-3 and pH-4 were retained as >90, >89, >88, and >88%, respectively, after 100 h. The results clearly revealed that hybrid composites exhibited higher temporal stability of γ_{33} values. It is suggested that the incorporation of polyimide into the inorganic materials could lead to better comprehensive properties especially higher stability. The better properties might be attributed to the existence of the fluorine in the side-chain of the polyimide and the formation of the silicon crosslinked network in the composite. Therefore, these results showed that these polymers might be useful in photonic device applications.

4. Conclusion

Nonlinear optical (NLO) polyimide containing silica inorganic/organic hybrids have been prepared by sol–gel method. The hybrids exhibit good thermal stability. They have network structure and silica particles were uniformly dispersed in the nanoscale. Covalent bonding (Si–O–Si) between the organic and the inorganic components enhanced miscibility. The prepared hybrids showed tunable refractive index with the silica fraction in the materials. Excellent optical transparence was obtained in the prepared materials. These results show that such hybrid thin films have potential applications as passive films for optical devices.

Acknowledgement

This work was financially supported by the Jiangsu Planned Projects for Postdoctoral Research Funds (0602037B), the Natural Science of Jiangsu Education (05KJB150016 and 06KJB510020) and the fund of Jiangsu University (06JDG015 and 06JDG076).

References

[1] Burland DM, Miller RD, Reiser O, Twieg RJ, Walsh CA. The design, synthesis, and evaluation of chromophores for second harmonic generation in a polymer waveguide. J Appl Phys 1992;71:410–7.
[2] Kobayashi Hiroaki, Kubo Masaki, Tsukada Takao, Hozawa Mitsunori. Numerical analysis for photothermal poling process of nonlinear optical polymer film. Int J Heat Mass Transfer 2002;45:865–75.
[3] Hikita M, Shuto Y, Amano M, Yoshimura R, Tomaru S, Kozawaguchi H. Optical intensity modulation in a vertically stacked coupler incorporating electro-optic polymer. Appl Phys Lett 1993;63:1161–3.
[4] Natansohn A, Rochon P, Gosselin J, Xie S. Azo polymers for reversible optical storage. Part 1. Poly[4′-[[2-(acryloyloxy)ethyl]ethylamino]-4-nitroazobenzene]. Macromolecules 1992;25:2268–73.
[5] Baek WS, Lee H. Photorefractive intermode spacecharge fields in volume holographic interconnections. J Appl Phys 1990;67:1194–202.
[6] Li Bo, Tong Rui, Zhu Rongyi, Meng Fanshun, Tian He, Qian Shixiong. The ultrafast dynamics and nonlinear optical properties of tribranched styryl derivatives based on 1,3,5-triazine. J Phys Chem B 2005;109(21):10705–10.
[7] Fanshun Meng, Jun Mi, Shixiong Qian, Kongchang Chen, He Tian. Linear and tri-branched copolymers for two-photon absorption and two-photon fluorescent material. Polymer 2003;44(22):6851–5.
[8] Chaumel Frederic, Jiang Hongwei, Kakkar Ashok. Sol–gel materials for second-order nonlinear optics. Chem Mater 2001;13:3389–95.
[9] Qiu Fengxian, Xu Hongliang, Cao Yonglin, Jiang Yan, Zhou Yuming, Liu Juzheng, et al. Nonlinear optical materials: synthesis, characterizations, thermal stability and electro-optical properties. Mater Charact 2007;58(3):275–83.
[10] Qiu Fengxian, Zhou Yuming, Liu Juzheng, Zhang Xuping. Preparation, morphological and thermal stability of polyimide/silica hybrid material containing dye NBDPA. Dyes Pigments 2006;71(1):37–42.
[11] Urlacher C, Marco De Lucas C, Mugnier J. Chemical and physical aspects of sol–gel process for planar waveguides elaboration; application to zirconia waveguides. Synth Met 1997;90:199–204.
[12] Qiu Fengxian, Cao Yonglin, Xu Hongliang, Jiang Yan, Zhou Yuming, Liu Juzheng. Synthesis and properties of polymer containing azo-dye chromophores for nonlinear optical applications. Dyes Pigments 2007;75(2):454–9.
[13] Leng WN, Zhou YM, Xu QH, Liu JZ. Synthesis of nonlinear optical side-chain soluble polyimides for electro-optic applications. Polymer 2001;42:7749–54.
[14] Qiu Feng-Xian, Zhou Yu-Ming, Liu Ju-Zheng. The synthesis and characteristic study of 6FDA–6FHP–NLO polyimide/SiO_2 nanohybrid materials. Eur Polym J 2004;40(4):713–20.
[15] Medda Samar Kumar, Kundu Debtosh, De Goutam. Inorganic–organic hybrid coating on polycarbonate: spectroscopic studies on the simultaneous polymerizations of methacrylate and silica networks. J Non-Cryst Solids 2003;318:149–56.

[16] Mascia L, Kioul A. Influence of siloxane composition and morphology on properties of polyimide–silica hybrids. Polymer 1995;36:3649–59.
[17] Tachibana H, Yamanaka Y, Sakai Y, Abe M, Matsumoto M. Highly conductive inorganic–organic hybrid Langmuir–Blodgett films based on MoS_2. Chem Mater 2000;12:854–6.
[18] Tsai MH, Whang WT. Low dielectric polyimide/poly(silsesquioxane)-like nanocomposite material. Polymer 2001;42:4197–207.
[19] Jiang Y, Cao ZQ, Shen QS, Dou XM, Chen YL. Improved attenuated-total-reflection technique for measuring the electro-optic coefficients of nonlinear optical polymers. J Opt Soc Am B 2000;17:805–8.